International Journal of Electrical and Computer Engineering (IJECE)
Vol. 7, No. 3, June 2017, pp. 1452~1458
ISSN: 2088-8708, DOI: 10.11591/ijece.v7i3.15150

Characterization of Defect Induced Multilayer Graphene

Marriatyi Morsin[1], Suhaila Isaak[2], Marlia Morsin[3], Yusmeeraz Yusof[4]
[1] Department of Polythecnic, Ministry of Education Malaysia, Presint 4, 62100 W.P Putrajaya, Malaysia
[1,2,4] Department of Electronic and Computer Engineering, Faculty of Electrical Engineering, Universiti Teknologi Malaysia, Johor Bahru, Johor, Malaysia
[3] Microelectronics and Nanotechnology – Shamsudin Research Center, Universiti Tun Hussein Onn Malaysia, Batu Pahat, Malaysia

Article Info

Article history:

Received Feb 8, 2017
Revised Apr 17, 2017
Accepted May 9, 2017

Keyword:

Multilayer graphene
Oxygen plasma
Raman spectroscopy
Reactive ion etching

ABSTRACT

A study of oxygen plasma on multilayer graphene is done with different flow rates. This is to allow a controlled amount of defect fabricated on the graphene. Results from the study showed that the intensity ratio of defect between D peak and G peak was strongly depended on the amount of oxygen flow rate thus affected the 2D band of the spectra. The inter-defect distance $L_D \geq 15$ nm of each sample indicated that low-defect density was fabricated. The surface roughness of the multilayer graphene also increased and reduced the conductivity of the multilayer graphene.

Corresponding Author:

Yusmeeraz Yusof,
Department of Electronic and Computer Engineering, Faculty of Electrical Engineering,
Universiti Teknologi Malaysia,
Johor Bahru, Johor, Malaysia.
Email: yusmeeraz@fke.utm.my

1. INTRODUCTION

Study about graphene defect has gained so much interest nowadays [1]–[3]. This is because of its two dimensional nature which makes it easier to add and remove carbon atoms so that it can fine-tune its electronic properties [3]. Several methods to introduce defect on graphene are atom bombardment [2], plasma treatment [4],[5], ion irradiation [6], focused e-beam [1] and pulse-voltage injection [7]. Among all techniques, plasma treatment is a common technique used to initiate defect.

Even though plasma etching is a common technique to introduce defect, however, many aspects of the disorder generated by this technique remain to be better understood especially in multilayer graphene. Study shows that oxygen plasma is very aggressive and usually results in drastic changes of the structural and electronic properties of graphene even at a short time of exposure [8].

Another important step after the introduction of defect is the characterization of the graphene surface. There are many instruments used for characterization and measuring defect on graphene including atomic force microscopy (AFM) [2],[9], high resolution transmission electron microscopy [10], transmission electron microscopy [1], scanning electron microscopy [10] and Raman spectroscopy [2],[6],[9],[11],[12]. Raman spectroscopy is more favorable since it is more sensitive and a non-destructive technique for investigating the properties of graphene. As reported by Guibai *et al*, AFM characterization makes no significant different between pristine and defected graphene, but not by using Raman [2].

In this study, different oxygen plasma flow rates are used in gradually inducing disorder in chemical vapor deposition (CVD) multilayer graphene and Raman spectroscopy is applied to cater the evolution of disorder. The intensity of the D, G and 2D bands in the Raman spectra are analyzed to explore the oxygen

plasma treatment effect in CVD multilayer graphene. The AFM characterization is used to study the morphology of the graphene samples while the electrical properties is done to cater the I-V characteristics of the samples.

2. RESEARCH METHOD

Initially the study sample was CVD multilayer graphene purchased from Graphene Supermarket.com. The 1 cm × 1 cm sample was then being diced into 0.5 cm × 0.5 cm respectively. Four different samples were used in this study. The samples were denoted by S1 – untreated CVD multilayer graphene, S2 – treated to 30 sccm oxygen flow rate, S3 – treated to 50 sccm oxygen flow rate and S4 - treated to 80 sccm oxygen flow rate.

In this experiment, dry etching using oxygen plasma treatment was carried out at room temperature. This treatment was done using the reactive ion etching (RIE) system capacitively coupled plasma (CCP) type discharged from SNTEK, model BEP5002 to fabricate the disorder on the CVD multilayer graphene. In this case, oxygen plasma was released and exposed directly to the CVD graphene multilayer surface. The parameters set for the oxygen plasma treatment were 30 sccm, 50 sccm and 80 sccm for the oxygen flow rates, 50 Watt power, 200 mTorr pressure and time of exposure of 5 s.

To study the crystallization structure of the untreated and the exposed graphene samples, Raman spectroscopy from Raman Xplora Plus, HORIBA Scientific with grating 1200 nm and visible wavelength 532 nm (2.33 eV in energy) with Nd Yag, laser type was used. The measurements were performed at room temperature. To be exact, only the exposed graphene area which was the center area were characterized.

The atomic force microscopy (AFM) (XE-100, Korea) was used to study morphology of the samples, and the 2-point probe from Keithley was used to measure the electrical property of the graphene device.

3. RESULTS AND ANALYSIS

3.1. Raman Characterization

Figure 1 (a) comparison of the 532 nm Raman spectra of graphene S1-S4. The figure shows three most intense features; which are the G-peak at ~ 1580 cm^{-1}, the 2D-peak at ~2700 cm^{-1} and the D-peak at ~1300 cm^{-1}. According to Zheng Jian *et al* the G-peak is due to the E_{2g} mode at the Γ- point [13]. The 2D-band or previously known as G' is in the range of 2500 – 2800 cm^{-1}; was a signature of graphitic sp^2 materials. The 2D band was also used in determining the number of layers of graphene [11],[13]. The D-band or as known as the disorder induced band which appeared at ~1345 cm^{-1} [14]. This band exhibited the presence of disorder in sp^2-hybridized carbon system results in resonance Raman spectra.

As shown in Figure 1 (a), sample S1, the untreated samples showed the slight appearance of D-peak which may be caused by the crystalline of the multilayer graphene during the production. As the samples were exposed to the oxygen gas plasma (O_2), the D-peak became intense. Although the disorder peak became intense, only a slight change happened to the 2D-band. This indicated that the graphene layers still existed.

Further investigation was done on the G and the D band. Based on Figure 1 (b), the D-peak increased intensely with the increasing amount of oxygen flow rate. The Raman spectra showed a slight D-peak at S1 sample to a strong D-peak for samples S2, S3 and S4. The G- peak did not show much difference relatively. Interestingly here, at S3 and S4 samples, the D'-peak started to arise at 1662 cm-1. As in Eckmann et al [11], the D'-peak may due to the existent of lattice defect. In opposition with the D'-peak, the D-peak was not sensitive to the defect geometry.

Figure 1 (c) shows the evolution of 2D-band. As mentioned earlier, the 2D-band is a signature of graphitic sp2 material. The 2D-band showed a broader band as studies show that multilayer graphene exhibit broadens 2D-band [13],[15]. The 2D-band of S2 and S4 showed symmetrical bell-shape but for S1, the 2D-band showed that the peak comprised with 2 component peaks in it. And there was a slight band shifting to the left on the S4 samples of the 2D-band. According to Zeng Jian et al [13] and Chih-Jen Shih *et al* [15], the spectra shape of S1 sample is mostly reflected to be thicker than 6- layers of graphene. Whilst for S2 and S4 samples, the spectra were mostly reflected 5 layers or less after comparing with the obtained 2D Raman spectra with the literature in [13],[16]. And for S3, the peak was small, so this peak may be reflected to less than 3 layers.

Another element can be retrieved from the 2D-band was the full width of half-maximum value. This value depended on the shape of the 2D-band where it was best run with the Lorentz peaks analysis. The Lorentz peaks analysis for S1, S2, and S4 were given the value of full width of half-maximum (FWHM) of 81.37 cm^{-1}, 76.38 cm^{-1}, and 64.39 cm^{-1}. But since the 2D peak for S3 was small, the FWHM could not be calculated. The D and G-band overshadowed the FWHM value of S3 2D-band. The cut down value of

FWHM confirmed the decreased layer of graphene. The small value of FWHM indicated the less layer of graphene [17].

The D, the G, and 2D peaks were useful to monitor the structural changes in graphene lattice and layers [8]. From Figure 1 (b) and Figure 1 (c) the intensity ratio of the D and G peaks I_D/I_G and that the ratio of 2D and G peaks I_{2D}/I_G as a function of oxygen plasma flow rate (sccm) can be calculated. The value of I_D and I_G was taken from the values of the peak intensity of the D-peak and the G-peak respectively to calculate the defect intensity ratio of the spectra. The I_D/I_G ratio was less than 0.20 for untreated S1 sample indicating the crystalline of the CVD multilayer graphene sample during the production. The I_D/I_G increased as the oxygen flow rate increased, indicating the increasing amount of defect. At short exposure time, the I_G was practically increased and remained constant afterward, while I_D strongly increased with oxygen plasma flow rate. While for I_{2D} the intensity decreased rapidly. This trend was expected as the Raman spectra have shown changing and shifting element on 2D- band and peak.

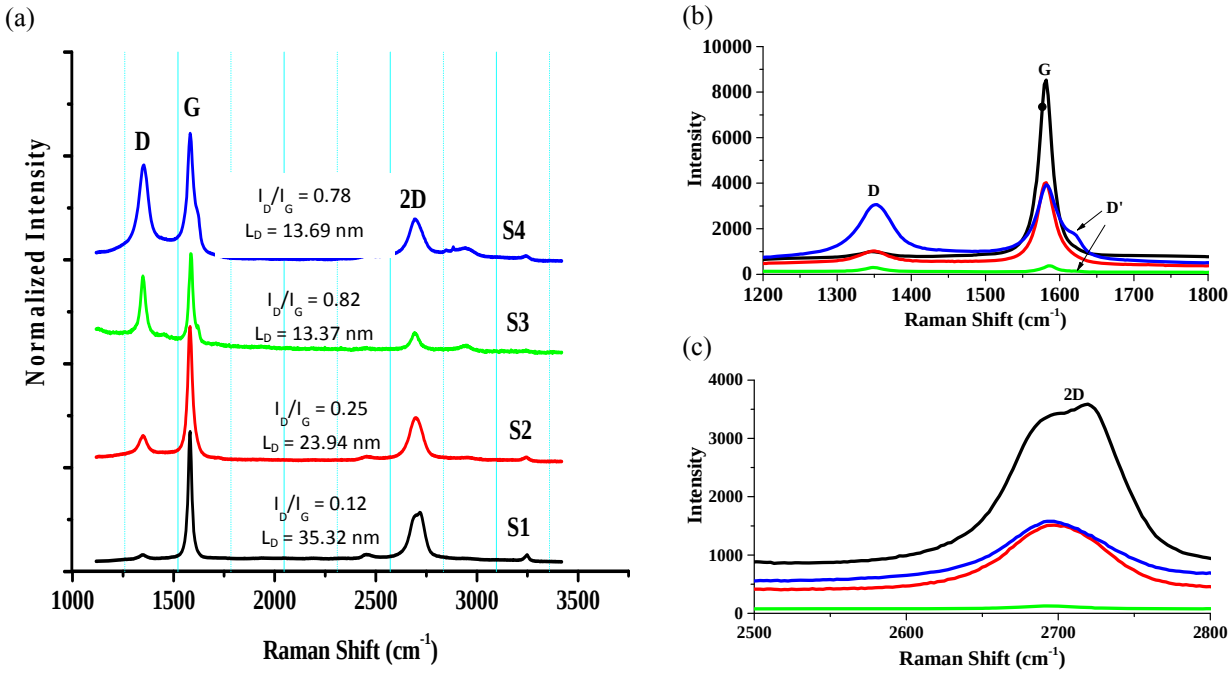

Figure 1. Evolution of the first-order and second-order Raman spectra for samples S1-S3 deposited on an SiO_2 substrate, subjected to the same oxygen plasma treatment with different amount of flow rates. (a) Comparison of Raman spectra at 532 nm for different doses of oxygen flow rates. (b) Evolution of G-peak and D-peak Raman spectra (c) Evolution of 2D-band at ~2650 cm^{-1}

**Note for Figure 1(b) and (c), the black colour Raman spectra is for S1, red colour Raman spectra is for S3, green colour Raman spectra is for S3, and blue colour Raman spectra is for S4.

The value of I_{2D}/I_G decreased when the value of I_D/I_G increased. A further calculation was done to classify the defect states using $I_D/I_{D'}$. Eckmann *et al* has classified two types of defect states which $I_D/I_{D'} > 7$ for sp^3-type defects and $I_D/I_{D'} < 7$ for vacancy defects [11]. In this study, only S4 sample exhibited the D'-peak, and the value of $I_D/I_{D'}$ was 1.84, which was in agreement of the formation of vacancy defect.

Other feature can be retrieved from this intensity ratio I_D/I_G was the distance of defect, L_D. Ado Jorio *et al* states that, in ion bombardment graphene, the disorder is better quantified by the defect concentration, $1/L_D^2$, where the L_D is a typical interdefect distance, with defect being a point-like (zero-dimensional) structure [12]. There are several equations related to calculating the L_D. One is from Cancado *et al* [18], for low-defect density regime;

$$L^2_D\,(nm^2) = (1.8 \pm 0.5) \times 10^{-9}\,\lambda^4_L\,(I_D/I_G)^{-1} \quad (1)$$

where in this case λ is 532 nm. The calculated L_D for S1, S2, S3 and S4 are 35.32 nm, 23.94 nm, 13.37 nm, and 13.69 nm respectively. Those values attributed to the gradual increase of I_D/I_G value for each sample.

And this L_D equation (1) is valid for Raman data using excitation wavelength in visible range which is obtained from graphene samples with point defect separated by $L_D \geq 10$ nm.

3.2. AFM Characterization

Figure 2 shows the AFM morphology of the non-treated and treated samples. The AFM morphology consists of 3-D image corresponding to each type of samples. The color of 3-D the peak (s) and the valley (s) of the graphene surface. The red and yellow color indicate the peak of the surface, whilst the green shows the flat surface, and the blue indicates the valleys or the deepest valley (s). Figure 2 for S1 we can see the qualitatively, the S1 shows the most homogenous peaks compared to other graphene samples exposed to the oxygen plasma treatment. The scattering amount of red colour (peak) dominated the surface of the graphene. Whilst for S2, S3 and S4, the amount of red peak diminished with the increased amount of oxygen flow rate.

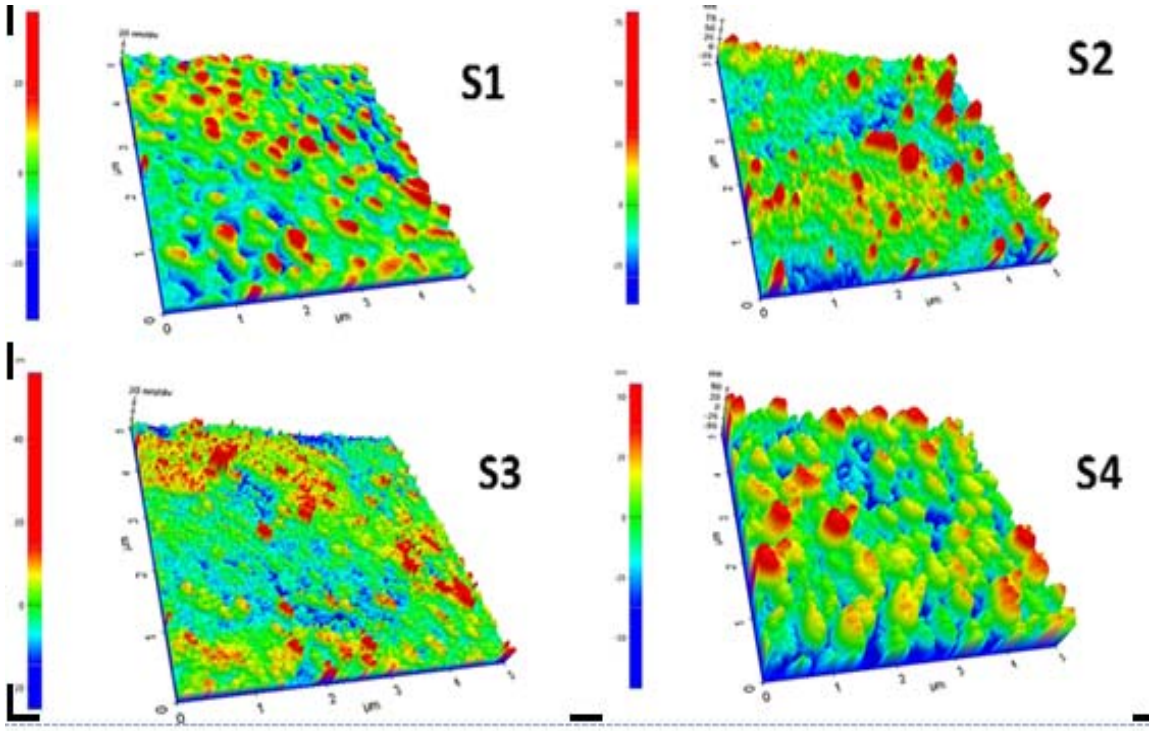

Figure 2. AFM analysis: three-dimensional (3-D) image corresponding to the x-axis of each samples

Table 1 is to conclude the relationships between the average surface roughness and the RMS roughness value of all samples.

Table 1. Comparison of roughness parameters for different oxygen plasma flow rate

Parameter	S1	S2	S3	S4
Average roughness (Ra.) in nm	6.79	11.45	5.77	15.28
Root mean square roughness (Rq) in nm	8.60	15.22	7.34	19.12

3.3. Electrical characterization

The current – voltage characteristics was done to gain more information about the effect of surface roughness due to oxygen plasma treatment. Figure 3 shows the current-voltage characteristic of the multilayer graphene with Al metal contact. It obviously showed that the multilayer graphene either in S1 or exposed to different doses of oxygen plasma exhibited ohmic behaviour. Among these samples, S1 showed the highest ohmic behavior compared to the other multilayer graphene device exposed samples. From this figure, the resistance of multilayer graphene device was strongly affected by the amount of flow rates of oxygen plasma, thus it decreased the conductance of the multilayer device. This finding was supported by the

study from K. Kim *et al* [18] which reported that the conductance of graphene device can be attributed to the structural defects introduced by the oxygen plasma.

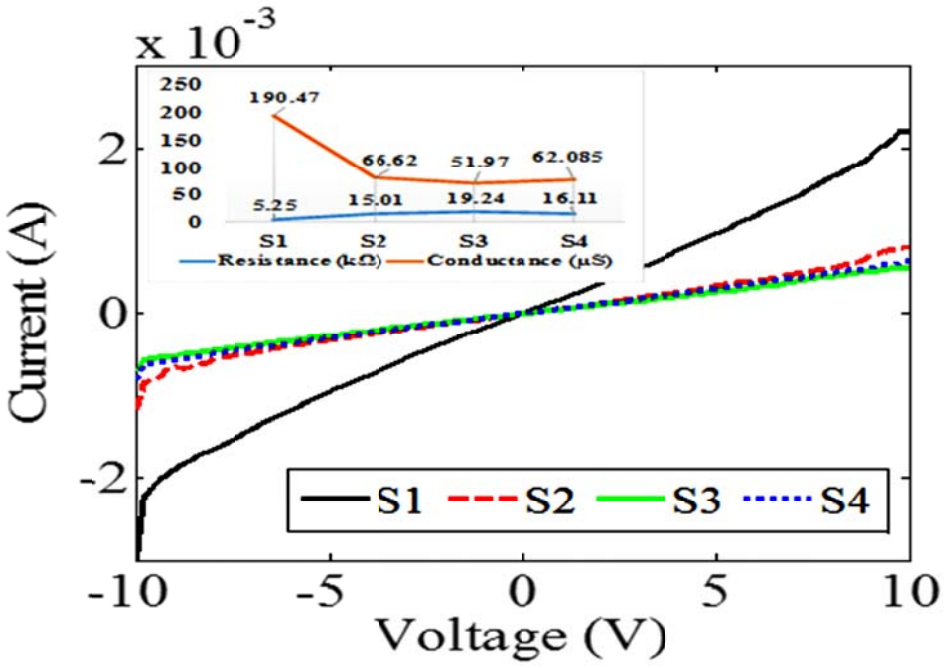

Figure 3. Current-voltage characteristics of multilayer graphene for pristine, 30 sccm, 50 sccm and 80 sccm respectively. Insert shows the values of resistance and conductance

4. CONCLUSION

The purpose of this study was to demonstrate the effect of the reactive ion etching using different controlled oxygen plasma flow rates on the CVD multilayer graphene. The defects fabricated on the graphene samples were then being characterized using the Raman spectroscopy, the AFM and the 2-point probe. From the study, it showed that the intensity ratio of I_{2D}/I_G decreased proportionally with the increased of the intensity ratio of I_D/I_G. The oxygen plasma flow rate also affected the 2D-band which represented the layer number of the graphene. From the values of I_D/I_G, the defect distance was also calculated which resulted in the low-defect-density distance of the samples. The oxygen plasma also gave impact to the surface roughness of the multilayer graphene. The increased amount of oxygen flow rates increased the surface roughness but lowered the conductivity of the multilayer graphene.

ACKNOWLEDGEMENTS

This research is funded by the Research University Grant of Universiti Teknologi Malaysia (UTM) under the Vote no. 12J10. The authors would like to thank the Research Management Centre of UTM and the Ministry of Higher Education Malaysia for their support and cooperation including students and other individuals who are either directly or indirectly involved in this project.

REFERENCES

[1] T. Xu, *et al.*, "Fabrication of nanopores using electron beam," *8th Annu. IEEE Int. Conf. Nano/Micro Eng. Mol. Syst.*, vol. 1, pp. 637–640, 2013.
[2] G. Xie, *et al.*, "A general route towards defect and pore engineering in graphene," *Small*, vol/issue: 10(11), pp. 2280–4, 2014.
[3] L. D. Carr and M. T. Lusk, "Graphene gets designer defects," *Nat. Publ. Gr.*, vol/issue: 5(5), pp. 316–317, 2010.
[4] A. Felten, *et al.*, "Gold clusters on oxygen plasma functionalized carbon nanotubes: XPS and TEM studies," *Nanotechnology*, vol/issue: 17(8), pp. 1954–1959, 2006.
[5] I. Childres, *et al.*, "Effect of oxygen plasma etching on graphene studied using Raman spectroscopy and electronic transport measurements," *New J. Phys.*, vol. 13, 2011.

[6] Y. Hajati, *et al.*, "Improved gas sensing activity in structurally defected bilayer graphene," vol. 505501.
[7] I. Yanagi, *et al.*, "Fabricating nanopores with diameters of sub-1 nm to 3 nm using multilevel pulse-voltage injection," *Sci. Rep.*, vol. 4, pp. 5000, 2014.
[8] A. Felten, *et al.*, "Controlled modification of mono- and bilayer graphene in O2, H2 and CF4 plasmas," *Nanotechnology*, vol/issue: 24(35), pp. 355705, 2013.
[9] G. Compagnini, *et al.*, "Ion irradiation and defect formation in single layer graphene," *Carbon N. Y.*, vol/issue: 47(14), pp. 3201–3207, 2009.
[10] Y. Yamada, *et al.*, "Subnanometer vacancy defects introduced on graphene by oxygen gas," *J. Am. Chem. Soc.*, vol/issue: 136(6), pp. 2232–5, 2014.
[11] A. Eckmann, *et al.*, "Probing the nature of defects in graphene by Raman spectroscopy," *Nano Lett.*, vol/issue: 12(8), pp. 3925–3930, 2012.
[12] A. Jorio, *et al.*, "Measuring Disorder in Graphene with Raman Spectroscopy," *Phys. Appl. Graphene - Exp.*, pp. 439–454, 2009.
[13] J. Zeng, *et al.*, "Irradiation effects of graphene and thin layer graphite induced by swift heavy ions," *Chinese Phys. B*, vol/issue: 24(8), pp. 1–7, 2015.
[14] M. M. Lucchese, *et al.*, "Quantifying ion-induced defects and Raman relaxation length in graphene," *Carbon N. Y.*, vol/issue: 48(5), pp. 1592–1597, 2010.
[15] C. J. Shih, *et al.*, "Bi- and trilayer graphene solutions Supporting Information," *Nat. Nanotechnol.*, vol/issue: 6(7), pp. 439–445, 2011.
[16] C. J. Lo, *et al.*, "Fabrication of symmetric sub-5 nm nanopores using focused ion and electron beams," *Nanotechnology*, vol/issue: 17(13), pp. 3264–3267, 2006.
[17] Y. Hao, *et al.*, "Probing layer number and stacking order of few-layer graphene by Raman Spectroscopy," *Small*, vol/issue: 6(2), pp. 195–200, 2010.
[18] L. G. Cancado, *et al.*, "Quantifying defects in graphene via Raman spectroscopy at different excitation energies," *Nano Lett.*, vol/issue: 11(8), pp. 3190–3196, 2011.

BIOGRAPHIES OF AUTHORS

Marriatyi Morsin received her Bachelor degree in Electrical Engineering (Biomedical Engineering) and Master degree at Universiti Teknologi Tun Hussein Onn (UTHM), Batu Pahat in 2002 and 2005. She is currently a Ph D.candidate in Faculty of Electrical Engineering at Universiti Teknologi Malaysia (UTM), Johor. Her research interests focus on defected graphene-based sensors.)

Suhaila Isaak received her Bachelor Degree in Electrical and Electronic Engineering from Universiti Teknologi Malaysia in 1998, the Master in Science (Electronic) degree from Universiti Putra Malaysia in 2001, and the Ph.D degree in Electrical and Electronics Engineering from University of Nottingham, England in 2011. Her major research interests are high-speed avalanche photodiodes and InP-GaAs photodetector design, simulation and fabrication. In addition, she is also working on integrated linear array photon camera using FPGA. Currently, she is involved on spectroscopy system for soil analysis.

Marlia Morsin was born in Malaysia in 1980. She received the B.Eng. degree in computer engineering from Universiti Technologi Malaysia (UTM) in 2002, the M.Eng. in electrical engineering from Universiti Tun Hussien Onn Malaysia (UTHM) in 2004 and the Ph.D. degree in microengineering and nanoelectronics from Universiti Kebangsaan Malaysia (UKM) in 2014. She joined University Tun Hussien Onn Malaysia (UTHM), Malaysia in 2004. Since 2004, she has been with Faculty of Electrical and Engineering, UTHM where she is currently a senior lecturer. Her main areas of research interest are nanomaterial and plasmonic sensor. Dr. Marlia is a Principal Researcher at Microelectronics & Nanotechnology - Shamsuddin Research Centre (MiNT-SRC), Institute of Integrated Engineering (I2E), Universiti Tun Hussein Onn Malaysia.

Yusmeeraz Yusof received the B.S. degree in electronics and the M.S. degree in integrated design engineering from Keio University, Japan, in 2002 and 2004, respectively, and the Ph.D. degree in electrical engineering and computer science from Nagoya University, Japan, in 2011. Before she joined Universiti Teknologi Malaysia (UTM) as a faculty member in 2006, she worked as an R&D engineer with Alps Electric Malaysia for two years. She is currently a Senior Lecturer with the Faculty of Electrical Engineering, UTM. Her current interests include CMOS DNA chip, semiconductor and new material biosensors, and point-of-care biomedical devices.